Report 3290

NAVAL SHIP RESEARCH AND DEVELOPMENT CENTER

Washington, D.C. 20007

DEPARTMENT OF THE NAVY · NAVAL SHIP R&D CENTER

FLAT PLATE FRICTIONAL DRAG REDUCTION

WITH POLYMER INJECTION

035

077

by

Justin H. McCarthy

This document has been approved for public release and sale; its distribution is unlimited.

DEPARTMENT OF HYDROMECHANICS

RESEARCH AND DEVELOPMENT REPORT

April 1970

Report 3290

FLAT PLATE FRICTIONAL DRAG REDUCTION WITH POLYMER INJECTION

The Naval Ship Research and Development Center is a U.S. Navy center for laboratory effort directed at achieving improved sea and air vehicles. It was formed in March 1967 by merging the David Taylor Model Basin at Carderock, Maryland and the Marine Engineering Laboratory (now Naval Ship R & D Laboratory) at Annapolis, Maryland. The Mine Defense Laboratory (now Naval Ship R & D Laboratory) Panama City, Florida became part of the Center in November 1967.

Naval Ship Research and Development Center
Washington, D.C. 20007

MAJOR NSRDC ORGANIZATIONAL COMPONENTS

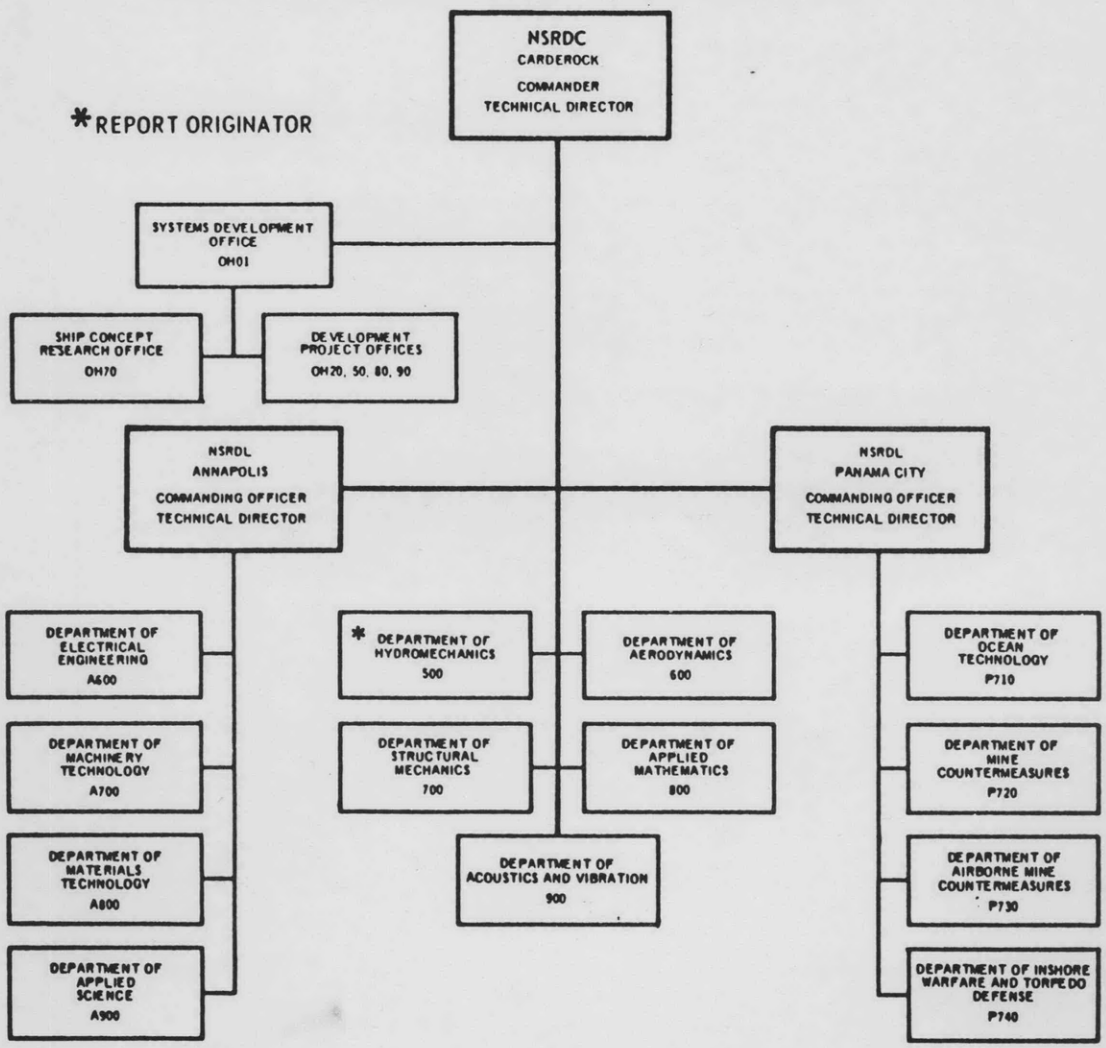

DEPARTMENT OF THE NAVY
NAVAL SHIP RESEARCH AND DEVELOPMENT CENTER
WASHINGTON, D. C. 20007

FLAT PLATE FRICTIONAL DRAG REDUCTION WITH POLYMER INJECTION

by

Justin H. McCarthy

April 1970

Report 3290

TABLE OF CONTENTS

LIST OF FIGURES

NOTATION

A	Reciprocal of von Kármán constant
$\Delta B \equiv B_{1_p} - B_{1_s}$	Friction reduction function
$B_1 = B_1\ (\ell^*, c)$	Function defined in Equation (2)
B_2	Constant defined in Equation (1)
$C_{F_x} \equiv \mathcal{D}_x / 1/2\ \rho_o\ U^2 x$	Frictional drag coefficient of plate
c	Uniform polymer concentration (parts per million by weight)
c_i	Concentration of polymer at injection
$c(x,y)$	Local polymer concentration
$c_x \equiv c(x,o)$	Polymer concentration at wall
D	Pipe diameter
$\mathcal{D}_x$	Frictional drag of one side of plate of length x
$f(\bar{y})$	Self-preservation velocity function defined in Equation (1)
ℓ	Polymer length scale
$M_i \equiv Q_i C_i / \alpha_1 \nu_2$	Defined in Equation (22)
$\mathcal{P}$	Integral defined by Equation (27)
$p(\bar{y})$	Self-preservation concentration function defined in Equation (22)
Q_i	Injected volume flow rate per unit of plate width
$R_x \equiv xU/\nu_o$	Reynolds number based on plate length
$R_\theta \equiv \theta U/\nu_o$	Reynolds number based on momentum thickness
U	Free-stream velocity past flat plate or average velocity at pipe centerline
$\bar{U}$	Pipe discharge velocity
$u \equiv u(x,y)$	Mean velocity in x-direction
$u_{\tau_x} \equiv \sqrt{\tau_{o_x}/\rho_o}$	Friction velocity
x	Distance measured along plate from leading edge
x_i	Injection location

x_j	Location of start of self-preserving concentration profiles ($x_j \geq x_i$)
y	Distance measured normal to plate
$\bar{y} \equiv y/\delta$	Nondimensional y
α_o	Constant defined above Equation (4)
α_1	Constant defined above Equation (22)
β_o	Constant defined above Equation (4)
β_1	Constant defined above Equation (22)
$\delta \equiv \delta_x \equiv \delta(x)$	Boundary layer thickness
$\theta \equiv \theta_x \equiv \theta(x)$	Momentum thickness
ν_o	Solvent kinematic viscosity
ρ_o	Solvent mass density
$\sigma_x \equiv U/u_{\tau_x}$	Local resistance parameter
$\tau_o \equiv \tau_{o_x} \equiv \tau_o(x)$	Wall shear stress

Subscript and Superscript

p	Evaluated for polymer solution
s	Evaluated for pure solvent
u	Evaluated for uniform polymer concentration
*	Length quantity nondimensionalized on u_{τ_x} and ν_o, as in $\ell^* \equiv \ell u_{\tau_x}/\nu_o$

ABSTRACT

A method is developed for prediction of frictional drag reduction in high Reynolds number flows past smooth flat plates with polymer injection near the leading edge. Numerical results are given for water-Polyox WSR 301 solutions with either uniform concentration or injection.

ADMINISTRATIVE INFORMATION

The work described in this paper was carried out at the Department of Hydromechanics of the Naval Ship Research and Development Center (NSRDC), and sponsored by the Naval Ship Systems Command (NAVSHIPS). Funding was under Subproject SF 35421003, Task 01710.

INTRODUCTION

The principal aim of the work reported here develops a method for analytical prediction of frictional drag reduction of smooth flat plates with polymer injection near the leading edge. The drag-reducing properties of certain dilute polymer solutions in turbulent flow are well known and previous studies[1,2] have treated the less practical problem of plate drag in polymer solutions of uniform concentration. The additional complication in injection problems is to account for polymer dilution in the turbulent boundary layer because local skin friction reduction appears to be strongly dependent on local polymer concentration at or near the wall.[3]

The treatment of the polymer injection problem presented here represents a straightforward extension of Granville's comprehensive formulation of the uniform polymer concentration problem.[1] For completeness, derivations of pertinent uniform concentration results are briefly outlined, along with some critical remarks on the several assumptions made. The velocity similarity laws carry over from the uniform to the nonuniform concentration case as a result of assuming that there is a local effective polymer concentration which is taken to be the local wall concentration.

---

[1]References are listed on page 23.

The ~~determination~~ of polymer dilution downstream of injection is based on the crucial assumption of self-preservation of concentration profiles, a notion first introduced to polymer problems by Fabula and Burns.[4] Throughout the development, which is restricted to high Reynolds number flows, the consistent approximation is made that terms of 0 $(1/\sigma)$, where $\sigma \equiv U/u_\tau$ is the local resistance parameter, may be neglected in comparison to terms of 0(1). Use of this approximation leads to relatively concise formulas which appear to offer conceptual and computational advantages when compared to similar work undertaken concurrently and independently by Granville.[5]

Computational methods are outlined which are suitable for hand calculation of frictional drag reduction of smooth flat plates in both uniform polymer concentration and polymer injection cases. In order to illustrate the methods, drag calculations have been performed for water solutions of Polyox WSR 301, one of the most effective drag-reducing polymers currently available. While the results of these calculations form an important part of this paper, their accuracy and significance are critically dependent on the experimentally determined values of the friction reduction function ΔB which have been used. Considerable additional fundamental experimental work is required to adequately "describe" ΔB for polymer solutions. At present, ΔB is a kind of unknown "black box" containing all the friction-reducing information for a given polymer solution, but it gives no information on the mechanism involved. Its virtue is that it permits development of a turbulent boundary layer theory which is a simple extension of that for ordinary Newtonian fluids.

UNIFORM POLYMER CONCENTRATION

VELOCITY SIMILARITY LAWS

Of the numerous works published on smooth wall turbulent boundary layers in dilute polymer solutions of uniform concentration, perhaps the most carefully argued theoretical analysis is that given by Granville.[1] His work may be viewed as a generalization of earlier Newtonian boundary layer theory based on dimensional analysis methods. As before, the boundary layer mean velocity profile is divided into three major regions: (1) a thin laminar sublayer where viscous effects dominate; (2) an inner transitional turbulent region, where both viscous and inertial effects are important and the effect of polymer is paramount; and (3) an outer turbulent region where inertial effects dominate and polymer effects are functionally unimportant. For the inner region, the polymer effect appears as a mean velocity dependence on polymer concentration by weight c and one (or more) polymer length scale(s) ℓ. As in the case of Newtonian turbulent boundary layers, for sufficiently high Reynolds numbers the inner and outer mean velocity profiles are assumed to coincide over some finite distance normal to the wall.

From such a picture, Granville deduces that the usual form of velocity defect law holds in the outer region

$$\frac{U-u}{u_\tau} = f(\bar{y}) \equiv - A \ln \bar{y} + B_2 - h(\bar{y}) \tag{1}$$

that the law of the wall in the overlapping part of the inner region is given by

$$\frac{u}{u_\tau} = A \ln y^* + B_1(\ell^*, c) \tag{2}$$

and that when the overlapping region exists

$$\sigma \equiv \frac{U}{u_\tau} = A \ln \delta^* + B_1(\ell^*, c) + B_2 \tag{3}$$

In the above the usual definitions apply, with $\bar{y} \equiv y/\delta$. A starred quantity is nondimensionalized by friction velocity $u_\tau \equiv \sqrt{\tau_o/\rho_o}$ and solvent viscosity ν_o, e.g., $\delta^* \equiv \delta u_\tau/\nu_o$. For pipe flow, $\delta = D/2$ is the pipe radius and U the mean velocity at the pipe centerline. For flat plate flow, $\delta \equiv \delta_x$ is the boundary layer thickness and U the free-stream velocity. The momentum thickness θ may be calculated to a high order of approximation by assuming that the velocity defect law, Equation (1), holds across the entire boundary layer. Then

$$\theta \equiv \int_o^\infty \frac{u}{U}\left(1 - \frac{u}{U}\right) dy = \frac{\delta}{\sigma}\, \alpha_o \left(1 - \frac{\beta_o}{\sigma}\right)$$

where

$$\alpha_o \equiv \int_0^\infty f(\bar{y})\, d\bar{y} \quad , \quad \beta_o \equiv \frac{1}{\alpha_o} \int_0^\infty f(\bar{y})^2\, d\bar{y}$$

Alternatively, one may write

$$R_\theta \equiv \frac{\theta U}{\nu_o} = \delta^* \alpha_o \left(1 - \frac{\beta_o}{\sigma}\right) \tag{4}$$

where

$$\delta^* = \exp\left\{\frac{1}{A}\left[\sigma - B_1(\ell^*,c) - B_2\right]\right\} \tag{5}$$

as follows from Equation (3).

The similarity laws given above are identical to those for a Newtonian fluid, except that B_1 is no longer a universal constant but depends on ℓ^* and c. The constants A and B_2 are respectively the reciprocal of the von Kármán constant, and the outer law constant appropriate to a particular flow boundary for a Newtonian fluid. The constancy of A and B_2 has been essentially verified by pipe flow velocity measurements for a variety of dilute polymer solutions.[6-8] For a particular type of polymer solution, B_1 (ℓ^*,c) is assumed to be a universal function which is independent of any particular flow boundary and must be determined by experiment. This assumption has never been verified experimentally, but it is fully analogous to the Newtonian fluid result, where B_1 has been experimentally shown to be a universal constant independent of flow boundary.

DETERMINATION OF ΔB

Perhaps the simplest experimental evaluation of B_1 (ℓ^*,c) is via the usual pipe flow measurements, making use of Equation (3) and the high order approximation $\sigma \cong \bar{U}/u_\tau$ + const, where $\bar{U}$ is pipe discharge velocity.[1] If Equation (3) is separately evaluated for pipe flow of a given Newtonian solvent (subscript s) and solvent-polymer combination (subscript p), it follows by subtraction that the "difference B_1," $\Delta B \equiv B_{1_p} - B_{1_s}$, is given by

$$\Delta B(\ell^*,c)_p = \left(\frac{\bar{U}_p}{u_{\tau_p}} - \frac{\bar{U}_s}{u_{\tau_s}}\right) + A \ln \frac{D_s^*}{D_p^*} \qquad (6)$$

From measurements of pipe discharge velocity and pressure drop, which is simply related to u_τ, ΔB may then be calculated from Equation (6). If ℓ/ν_{o_p} is assumed to be a constant independent of temperature for a given type of polymer solution, then ΔB should theoretically correlate with u_{τ_p} and c. In fact, most of the available pipe data indicate that ΔB does correlate reasonably well with u_{τ_p} and c if the pipe Reynolds number and radius (i.e., boundary layer thickness) are sufficiently large.[9-11] Since ℓ is physically undefined and ν_{o_p} is strongly dependent on temperature, further experiments over a wider range of temperatures than previously used are required to definitively establish that ΔB correlates with u_{τ_p}. For a fixed temperature, no distinctions can be made. The theoretical dependence of ΔB on $\ell^* \equiv \ell u_\tau/\nu_o$ is of course not unique, and the theory could easily be altered to accommodate a different nondimensional dependence on u_τ without introducing any significant changes in subsequent theoretical deductions.

The boundary layer thickness effect on ΔB mentioned above can not be considered resolved. For many polymer-solvent types, additional carefully conducted experiments are required for a greater range of pipe diameters, polymer concentrations, and higher wall shear stresses than previously tried. A rough theoretical treatment of the extent of the pipe diameter-Reynolds number effect may be found in Granville's discussion of minimum pipe required for the logarithmic law of the wall,[1] Equation (2).

For the high wall shear stresses to be considered here, the only experimental data available for calculation of ΔB for water-Polyox WSR 301 solutions are those obtained by Fabula in 1965.[12] His data were obtained in a smooth pipe of 1-cm diameter at temperatures in the range 73-82 F for polymer concentrations up to 66 ppm. Using Equation (6), ΔB has been evaluated from these data and is plotted in Figure 1 as a function of wall shear stress τ_o for constant values of concentration. Figure 2 shows a

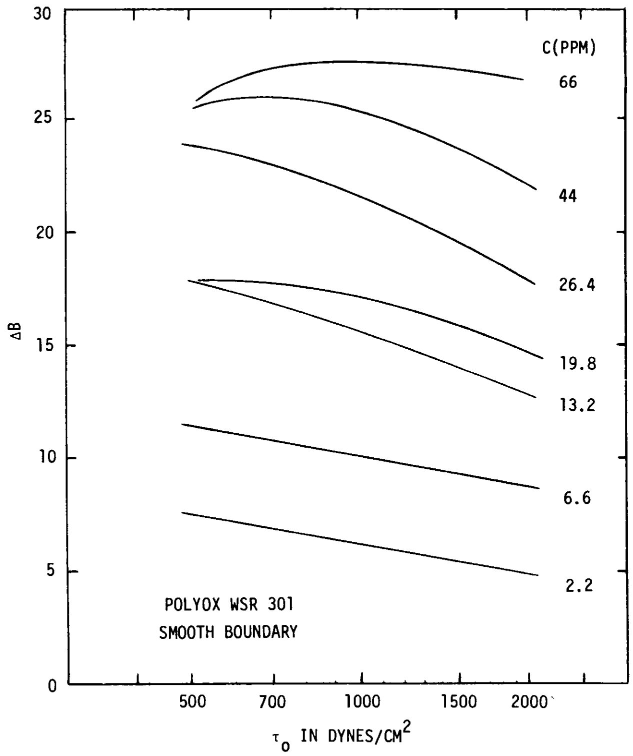

Figure 1 - Values of ΔB Obtained from Smooth Pipe Flow Tests at 73-82 F

(From Reference 12)

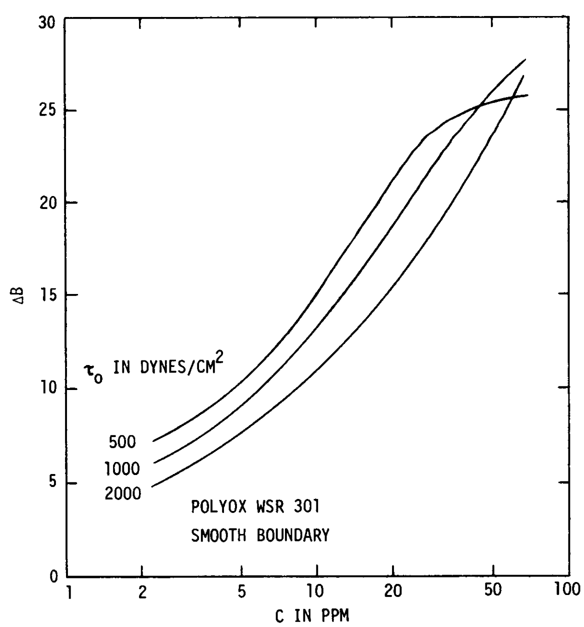

Figure 2 - Cross-Plot of Figure 1

cross-plot for constant values of shear stress. It will be assumed here as a working hypothesis that the pipe diameter effect on ΔB is negligible and that ΔB correlates with τ_o and c. (Correlation with τ_o is roughly equivalent to correlation with u_τ since ρ_o varies little with temperature.) These assumptions are certainly questionable, but there appears to be little or no rational basis for doing otherwise.

It can not be emphasized too strongly that the greatest uncertainty in any calculation of drag reduction for polymer solutions arises from uncertainty about the values of ΔB used. This is vividly illustrated by Fabula's[2] plots of different ΔB values for Polyox WSR 301 at low shear stresses experimentally determined by Virk,[8] Fabula,[12] and Goren.[13] Some but not all of the uncertainty arises from possible diameter and temperature effects. Other reasons for uncertainty arise from the molecular variability of different batches of ostensibly the same polymer, different polymer handling and mixing methods which result in unknown polymer degradation, different mechanical degradation of polymer coils dependent on pipe length to measurement sections, and the quality of equipment used and the care with which the ΔB experiments are carried out.

FLAT PLATE FRICTIONAL DRAG

In the case of two-dimensional flow of polymer solution parallel to a flat plate, shear stress and momentum thickness are related by the equation

$$\frac{d\,\theta_x}{dx} = \sigma_x^{-2} \tag{7}$$

This is the usual result obtained by integration of the momentum equations, use of the continuity equation, and neglect of the normal Reynolds stresses and streamwise variation in direct stress. The frictional drag coefficient C_{F_x} of one side of the plate up to distance x from the leading edge is then given by

$$C_{F_x} \equiv \frac{\mathcal{D}\,x}{1/2\,\rho_o\,U^2 x} = \frac{2}{x}\int_o^x \sigma_{x'}^{-2}\,dx' = 2\,\frac{R_{\theta_x}}{R_x} \tag{8}$$

which together with Equation (4) implies

$$\delta_x^* = \frac{C_{F_x} R_x}{2\ \alpha_o} \left(1 - \frac{\beta_o}{\sigma_x}\right)^{-1} \tag{9}$$

Substitution into Equation (3) leads to the following relation between C_{F_x} and σ_x:

$$\ln\left(R_x\ C_{F_x}\right) = \frac{1}{A}\left[\sigma_x - B_1(\ell^*, c)\right] + \ln\left[2\alpha_o\left(1 - \frac{\beta_o}{\sigma_x}\right)\right] - \frac{B_2}{A} \tag{10}$$

To determine C_{F_x}, an additional equation relating C_{F_x} and σ_x must be obtained. Following Granville,[1] integration of Equation (7) by parts gives

$$R_x = \sigma_x^{\ 2}\ R_{\theta_x} - 2 \int_o^x R_{\theta_{x'}}\ \sigma_{x'}\ \frac{d\ \sigma_{x'}}{dx'}\ dx'$$

or, equivalently, making use of Equations (4) and (8),

$$\frac{2}{C_{F_x}} = \sigma_x^{\ 2} - \frac{2\ \alpha_o}{R_{\theta_x}} \int_o^x \delta^*_{x'}\left(1 - \frac{\beta_o}{\sigma_{x'}}\right)\sigma_{x'}\ \frac{d\ \sigma_{x'}}{dx'}\ dx'$$

Substitution of Equation (5) for $\delta^*_{x'}$ and another integration by parts eventually leads to

$$\frac{2}{C_{F_x}} = \sigma_x^{\ 2} - 2A\ \sigma_x \frac{\left(1 - \dfrac{A+\beta_o}{\sigma_x}\right)}{\left(1 - \dfrac{\beta_o}{\sigma_x}\right)} - \frac{2\ \alpha_o}{R_{\theta_x}} \int_o^x \delta^*_{x'}\ \sigma_{x'}\left(1 - \frac{A+\beta_o}{\sigma_{x'}}\right)\frac{d\ B_1}{dx'}\ dx' \tag{11}$$

Now, if for convenience, one takes $B_1 = B_1\ (\ln\ \ell^*,\ \ln\ c)$, it follows that for the case of uniform concentration

$$\frac{d\ B_1}{dx} = -\frac{1}{\sigma}\ \frac{\partial\ B_1}{\partial \ln\ \ell^*}\ \frac{d\sigma}{dx}$$

Substitution into the integral of Equation (11), use of Equation (5), and repeated integration by parts results in

$$\frac{2}{C_{F_x}} = \sigma_x^{\,2} - 2A\,\sigma_x + 2A\left(A + \left.\frac{\partial B_1}{\partial \ln \ell^*}\right|_x\right) + \text{terms of } 0\left(\frac{1}{\sigma_x}\right) \text{ and higher}$$

For high Reynolds number flows, $R_x \equiv Ux/\nu_o > 10^7$, $A/\sigma_x << 1$ and normally $1/\sigma_x^{\,n}|\partial^n B_1/\partial \ln \ell^{*n}| << 1$, so that one obtains the high order approximation

$$\frac{2}{C_{F_x}} \cong \sigma_x^{\,2} - 2A\,\sigma_x \tag{12}$$

Alternatively

$$\sigma_x \equiv \frac{U}{u_{\tau_x}} \cong \sqrt{\frac{2}{C_{F_x}}} + A \tag{13}$$

which upon substitution into Equation (10) finally gives an equation for C_{F_x}

$$\ln\left(R_x\, C_{F_x}\right) \cong \frac{1}{A}\left[\sqrt{\frac{2}{C_{F_x}}} - B_1\,(\ell_x^*, c)\right] + \text{const} \tag{14}$$

Equations (12) to (14), which hold only for polymer solutions of uniform concentration, are identical in form to those for a Newtonian fluid. These equations show that in the case of uniform concentration, to a high degree of approximation, the frictional drag reduction is controlled only by the value of $B_1(\ell^*, c)$ at the trailing edge. Changes in B_1 along the length of the plate caused by changes in shear stress (ℓ_x^*), have negligible effect on drag. This is a key result and permits a major simplification of the computation of drag.

A convenient scheme for calculation of plate frictional drag in uniform polymer solution may be obtained as follows. If Equation (14) is separately evaluated for flat plate flow of a given Newtonian solvent (subscript s) and solvent-polymer combination (subscript p), it follows by subtraction and rearrangement that

$$\sqrt{\frac{2}{\left(C_{F_x}\right)_s}}\left[\sqrt{\frac{\left(C_{F_{x\,s}}\right)}{\left(C_{F_{x\,p}}\right)}}-1\right] + A \ln\left[\frac{\left(R_x\right)_s}{\left(R_x\right)_p}\,\frac{\left(C_{F_x}\right)_s}{\left(C_{F_x}\right)_p}\right] = \Delta B\left[\left(\ell_x{}^*\right)_p\,,\,c\right] \tag{15}$$

Similarly, from Equation (13), it is easily shown that

$$\frac{U_s}{U_p} \cong \frac{\left(u_{\tau_x}\right)_s}{\left(u_{\tau_x}\right)_p}\sqrt{\frac{\left(C_{F_x}\right)_p}{\left(C_{F_x}\right)_s}} \tag{16}$$

when terms of $0\left(\sqrt{C_{F_x}}\right)$ and higher are neglected. Substitution into the Reynolds number quotient of Equation (15) gives

$$\sqrt{\frac{2}{\left(C_{F_x}\right)_s}}\left[\sqrt{\frac{\left(C_{F_x}\right)_s}{\left(C_{F_x}\right)_p}}-1\right] + A \ln\left[\frac{x^*_s}{x^*_p}\sqrt{\frac{\left(C_{F_x}\right)_s}{\left(C_{F_x}\right)_p}}\right] = \Delta B\left[\left(\ell_x{}^*\right)_p\,,\,c\right] \tag{17}$$

where $x^* \equiv x\, u_{\tau_x}/\nu_o$. Now, $\left(C_{F_x}\right)_s$ is a known function of $\left(R_x\right)_s$. Thus for fixed values of x and ν_o (i.e., $x_p = x_s = x$, $\nu_{o_p} = \nu_{o_s} = \nu_o$), and specified U_s, $\left(C_{F_x}\right)_s$ is known, and $\left(u_{\tau_x}\right)_s$ may be determined from Equation (13). Setting $\left(u_{\tau_x}\right)_p = \left(u_{\tau_x}\right)_s = u_{\tau_x}$, Equation (17) reduces to

$$\sqrt{\frac{2}{\left(C_{F_x}\right)_s}}\,(\xi-1) + A \ln \xi = \Delta B\left(\frac{\ell}{\nu_o}\,u_{\tau_x}\,,\,c\right) \tag{18}$$

where

$$\xi \equiv \sqrt{\frac{\left(C_{F_x}\right)_s}{\left(C_{F_x}\right)_p}}\;\Bigg|\left(x,\,\nu_o,\,u_{\tau_x}\,,\,c\right) = \text{const}$$

For the known $\left(C_{F_x}\right)_s$ and experimentally determined values of ΔB, this equation is easily solved for ξ, from which $\left(C_{F_x}\right)_p$ follows. The corresponding $\left(R_x\right)_p$ follows from Equation (16) and is given by

$$\left(R_x\right)_p = \xi \left(R_x\right)_s \tag{19}$$

Calculations of $\left(C_{F_x}\right)_p$ and $\left(R_x\right)_p$ were carried out according to the above scheme for salt water solutions of Polyox WSR 301 over the range of friction velocities and concentrations for which ΔB data are shown in Figures 1 and 2. The value of A was taken to be 2.39, and a reference temperature of 59 F was used. The results are shown in Figure 3 for plate lengths of 10, 100, and 400 ft. The zero concentration C_{F_x} versus R_x curve was obtained from the tabulation given in Reference 14. For each plate length and all nonzero concentrations but the highest, $\left(C_{F_x}\right)_p$ is seen to increase with increasing R_x. This is a direct result of the fact that ΔB decreases with increasing friction velocity for the range of friction velocities covered in Figure 1. At sufficiently high Reynolds numbers (and friction velocities), the $\left(C_{F_x}\right)_p$ curves will presumably intersect the $\left(C_{F_x}\right)_s$ curve, yielding no drag reduction.

The percentage reductions in frictional drag may be easily computed as a function of concentration from the curves shown in Figure 3. The results are plotted in Figure 4 for the three plate lengths at flow speeds of 20, 30, and 40 knots. For the range of variables considered, it is seen that the percentage drag reduction (1) increases with increasing concentration, apparently reaching a maximum at some concentration greater than 30 ppm, dependent on length and speed; (2) decreases with increasing speed, up to concentrations of about 70 ppm; and (3) decreases as the length increases from 10 to 100 ft and remains the same for greater lengths. At the higher speeds and at concentrations less than about 30 ppm, the length effect is generally small.

POLYMER INJECTION (NONUNIFORM CONCENTRATION)

VELOCITY SIMILARITY LAWS

The velocity similarity laws for uniform polymer concentration, Equations (1) and (2), may be rederived for the case of nonuniform concentration by making the additional assumption that there is an effective polymer concentration $c_e(x)$ independent of distance from the wall. The same similarity laws still hold, taking $B_1 = B_1$, (ℓ_x^*, c_{e_x}). Since the

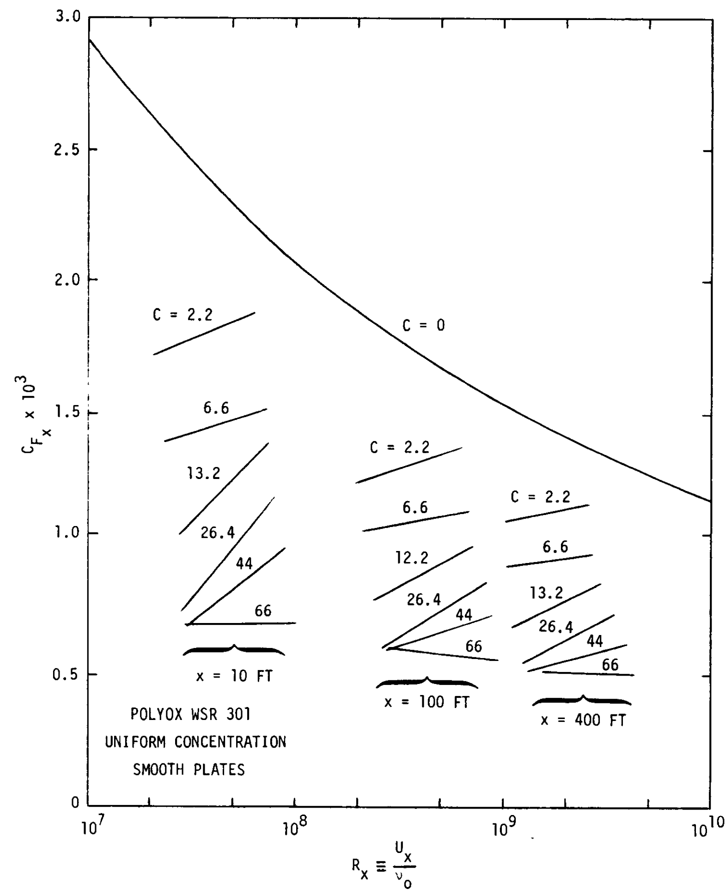

Figure 3 - Predicted Frictional Drag Coefficients of Smooth Flat Plates in Solutions of Uniform Concentration

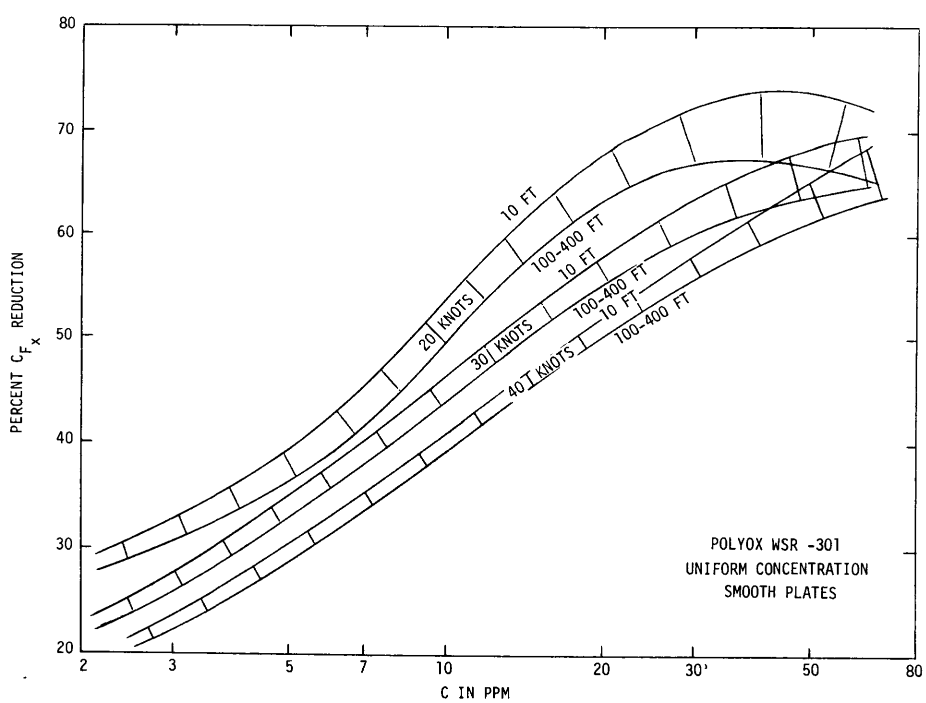

Figure 4 - Predicted Percentage Frictional Drag Reduction Derived from Figure 3

presence of polymer directly affects only the law of the wall, Equation (2), it will be assumed that $c_{e_x} = c_x$, where c_x is the concentration at the wall. This assumption is consistent with experiments on polymer injection at the centerline of a pipe, which indicate that wall shear stress reduction does not occur until polymer diffuses into the wall region.[3] It follows from this assumption that Equations (1) through (11), derived for uniform polymer concentration, are also valid for nonuniform concentration when B_1 is given by $B_1 = B_1\ (\ell_x^*, c_x)$. In principle then, it remains only to determine the variation of polymer concentration along the wall.

A simple but interesting result follows from the above assumptions. For a given speed U and given polymer type, the frictional drag of a flat plate depends only on the values of wall shear stress ℓ_x^* or σ_x and wall concentration c_x at the trailing edge; the drag is independent of whether the concentration is uniform or nonuniform upstream of the trailing edge. This result follows immediately from Equation (10), which is valid for both uniform and nonuniform concentrations when one takes $B_1 = B_1\ (\ell_x^*, c_x)$. Generally of course, two plates traveling at speed U, one with uniform concentration and the other with nonuniform concentration, can have equal trailing edge shear stresses and wall concentrations (and drags) only if their lengths are different. This is physically obvious since the drag-reducing parameter ΔB is strongly dependent on concentration, and it also follows from the constraints which will be imposed by Equations (31) through (36).

POLYMER DILUTION

If polymer solution is injected into a flat plate turbulent boundary layer from a line source located in the plate at $x = x_i$, the existing turbulent motions will rapidly distribute polymer throughout the boundary layer. As a result, the concentration of polymer near the wall can be expected to decrease with increasing distance downstream of the injection location, and drag predictions must account for this variable concentration. For steady, two-dimensional flow of incompressible dilute polymer solutions with negligible molecular diffusion, polymer concentration is governed by its mass balance equation, which when integrated gives

$$Q_i \; c_i = \int_0^\infty u(x,y) \; c(x,y) \; dy \tag{20}$$

independent of x. Q_i and c_i are respectively the injected volume flow rate per unit plate width and the injected polymer concentration. Equation (20) will be assumed to hold for turbulent boundary layers, taking u and c as mean values. As argued by Fabula and Burns, negligible error is introduced by this assumption if the fluctuations of u and c are small compared to their mean values.[4]

For sufficiently large distances downstream of the injection location, say $x \geq x_j \geq x_i$, it might be expected that the polymer plume will more than fill the boundary layer and that the concentration profiles will have a self-preserving form given by

$$c(x,y) = c_x \; p(\bar{y}) \quad , \quad x \geq x_j \tag{21}$$

where $c_x \equiv c(x,o)$. Using earlier diffusion studies by Poreh and Cermak,[15] Fabula and Burns were the first to introduce the notion of self-preservation of concentration profiles in polymer injection problems. They found that an exponential representation for $p(\bar{y})$ yielded good correlation of polymer concentrations measured by Wetzel and Ripken[16] in a channel boundary layer. As in the case of uniform polymer concentration, it is to be expected that the velocity defect law, Equation (1), holds across most of the boundary layer. Thus, for the self-preserving region, substitution of Equations (1) and (21) into (20) gives the high order approximation

$$Q_i \; c_i = \alpha_1 \; U \; \delta_x \; c_x \left(1 - \frac{\beta_1}{\sigma_x}\right) \; , \quad x \geq x_j$$

where

$$\alpha_1 \equiv \int_0^\infty p(\bar{y}) \; d\bar{y} \quad , \quad \beta_1 \equiv \frac{1}{\alpha_1} \int_0^\infty p(\bar{y}) \; f(\bar{y}) \; d\bar{y}$$

and $c_x \equiv c(x,o)$. Equivalently, one may write

$$M_i \equiv \frac{Q_i\ c_i}{\alpha_1\ \nu_o} = \delta_x^*\ \sigma_x\ c_x \left(1 - \frac{\beta_1}{\sigma_x}\right), \qquad x \geq x_j \tag{22}$$

which is the final form of the equation governing polymer concentration at the wall for the self-preserving region.

No such simple picture emerges for the intermediate mixing region $x_i \leq x \leq x_j$, where the polymer plume is rapidly thickening to fill the boundary layer immediately following injection. In an effort to carry over the idea of self-preservation to this intermediate region, the most one might expect is that

$$c(x,y) = c_x\ g\left(\frac{y}{\lambda(x)}\right), \qquad x_i \leq x \leq x_j$$

where y is normalized on some characteristic plume thickness $\lambda(x)$ rather than on the boundary layer thickness $\delta(x)$. Alternatively, setting $m(x) \equiv \lambda(x)/\delta(x)$, one may write

$$c(x,y) = c_x\ g\left(\frac{\bar{y}}{m(x)}\right), \qquad x_i \leq x \leq x_j \tag{23}$$

To be consistent with Equation (21) $m(x)$ must be constant for $x \geq x_j$. Such a representation has been found adequate for all but the initial part of the intermediate region when a passive material is injected into a turbulent boundary layer.[14]

If Equation (23) is assumed to also hold for nonpassive polymer injection, it is easily seen that the wall concentration in the intermediate region is governed by an equation of the same form as (22), except that α_1 and β_1 are now functions of x. The main problem then would be to specify $m(x)$. It is unlikely that an $m(x)$ determined for passive material injection would be appropriate for polymer injection, since generally the introduction of polymer will significantly alter the boundary layer in the intermediate region. The form of $m(x)$ will also depend on the injection method and location on a body.

For high Reynolds number flows, if attention is restricted to the case of polymer injection near the leading edge where the boundary layer is turbulent and thin, the length of the intermediate region may be expected to be small compared to the body length. In this case small error will be introduced in the calculation of frictional drag by assuming that no intermediate region exists and that the self-preserving concentration region begins immediately upon injection (i.e., $x_j = x_i$). After further justification, this assumption will eventually be made here. For the time being, we proceed without the assumption.

FLAT PLATE FRICTIONAL DRAG

As in the case of uniform concentration, two equations are available to relate C_{F_x} and σ_x, namely Equations (10) and (11). If for convenience one takes $B_1 = B_1 (\ln \ell_x^*, \ln c_x)$, it follows that

$$\frac{d B_1}{dx} = \begin{cases} 0 & , \; x < x_i \\ -\dfrac{1}{\sigma_x} \dfrac{\partial B_1}{\partial \ln \ell_x^*} \dfrac{d \sigma_x}{dx} + \dfrac{1}{c_x} \dfrac{\partial B_1}{\partial \ln c_x} \dfrac{d c_x}{dx} & , \; x \geq x_i \end{cases}$$

which may be used to evaluate the integral on the right side of Equation (11). But, as noted in the case of uniform concentration, the variation of B_1 with shear stress (i.e., ℓ_x^*) gives a negligible contribution to the equation, so that to a high degree of approximation one may take

$$\frac{d B_1}{dx} \cong \begin{cases} 0 & , \; x < x_i \\ \dfrac{1}{c_x} \dfrac{\partial B_1}{\partial \ln c_x} \dfrac{d c_x}{dx} & , \; x \geq x_i \end{cases} \qquad (24)$$

Substitution of Equations (4) and (24) into Equation (11) and neglect of higher order terms readily leads to

$$\frac{2}{C_{F_x}} \cong \sigma_x^{\,2} - 2A\,\sigma_x - \frac{2}{\delta_x^*} \int_{x_j}^{x} \frac{\delta^*_{x'}\,\sigma_{x'}}{c_{x'}} \frac{\partial B_1}{\partial \ln c_{x'}} \frac{d c_{x'}}{dx'}\, dx' + \mathcal{R} \qquad (25)$$

where

$$\mathcal{R} \equiv - \frac{2}{\delta_x^*} \int_{x_i}^{x_j} \frac{\delta_{x'}^* \sigma_{x'}}{c_{x'}} \frac{\partial B_1}{\partial \ln c_{x'}} \frac{d c_{x'}}{dx'} dx'$$

is the polymer contribution to the integral in the intermediate mixing region.

By use of Equation (22), which gives the wall concentration in the self-preserving region, Equation (25) reduces to

$$\frac{2}{C_{F_x}} \cong \sigma_x^{2} - 2 \sigma_x (A - \mathcal{P}) + \mathcal{R} \tag{26}$$

where

$$\mathcal{P} \equiv - c_x \int_{x_j}^{x} \frac{1}{c_{x'}^2} \frac{\partial B_1}{\partial \ln c_{x'}} \frac{d c_{x'}}{dx'} dx' \tag{27}$$

If c_x is assumed to decrease monotonically with increasing x, as seems physically reasonable, c_x may be taken as the independent variable in the $\mathcal{P}$ integral, so that

$$\mathcal{P} = c_x \int_{c_x}^{c_{x_j}} \frac{1}{c_{x'}^2} \frac{\partial B_1}{\partial \ln c_{x'}} d c_{x'} \tag{28}$$

Alternatively, if B_1 is an analytic function of c_x, then repeated integration by parts of (27) yields the series result

$$\mathcal{P} = \sum_{m=1}^{\infty} \left(\left. \frac{\partial^m B_1}{\partial \ln c_{x'}^{\,m}} \right|_x - \frac{c_x}{c_{x_j}} \left. \frac{\partial^m B_1}{\partial \ln c_{x'}^{\,m}} \right|_{x_j} \right) \tag{29}$$

For polymer injection near the leading edge, with $x_j/x \ll 1$, we expect that $c_x/c_{x_j} \ll 1$. If $\partial B_1/\partial \ell n\, c$ does not vary greatly with c and ℓ^*, it then follows from Equation (28) or (29) that the major polymer contribution to the $\mathcal{P}$ integral occurs towards the trailing edge of the plate. That this is true for Polyox solutions is demonstrated in Figure 5, which shows $1/c^2 \; \partial B_1/\partial \ln c$ versus c, for τ_o in the range 700 to 1300 dynes/cm.^{2} (Figure 5 is derived from Figure 2.) If the above result is qualitatively extended to the intermediate mixing region, for $x_i/x \ll 1$ and $\left(x_j - x_i\right)/x \ll$ one expects that $\mathcal{R}$ will be small relative to the other terms appearing in Equation (26). Subject to the restrictions outlined above, it will be assumed that $x_j = x_i$ so that $\mathcal{R} = 0$. Then, by Equations (26) and (28)

$$\frac{2}{C_{F_x}} \cong \sigma_x^{\;2} - 2\,\sigma_x\,(A - \mathcal{P}) \tag{30}$$

or alternatively

$$\sigma_x \cong \sqrt{\frac{2}{C_{F_x}}} + (A - \mathcal{P}) \tag{31}$$

where

$$\mathcal{P} \cong c_x \int_{c_x}^{c_{x_i}} \frac{1}{c_{x'}^{\;2}} \, \partial \left.\frac{\partial B_1}{\ln c_{x'}}\right|_{\ell_x^*} dc_{x'} \tag{32}$$

Substitution of Equation (31) into (10) finally gives the drag equation

$$\ell n\left(C_{F_x} R_x\right) \cong \frac{1}{A}\left[\sqrt{\frac{2}{C_{F_x}}} - B_1\left(\ell_x^*, c_x\right) - \mathcal{P}\right] + \text{const} \tag{33}$$

which differs from the uniform concentration case, Equation (14), only by the $\mathcal{P}$ integral. To the same order of approximation, the wall concentration is governed by

$$M_i \equiv \frac{Q_i\, c_i}{\alpha_1\, \nu_o} \cong \frac{\left(C_{F_x} R_x\right)}{2\,\alpha_o}\,\sigma_x\, c_x\,, \quad x \geq x_i \tag{34}$$

which follows from Equations (22) and (9). For given c_x and τ_{o_x} (i.e., ℓ_x^*), $\mathcal{P}$ may be evaluated from (32) provided c_{x_i} can be specified.

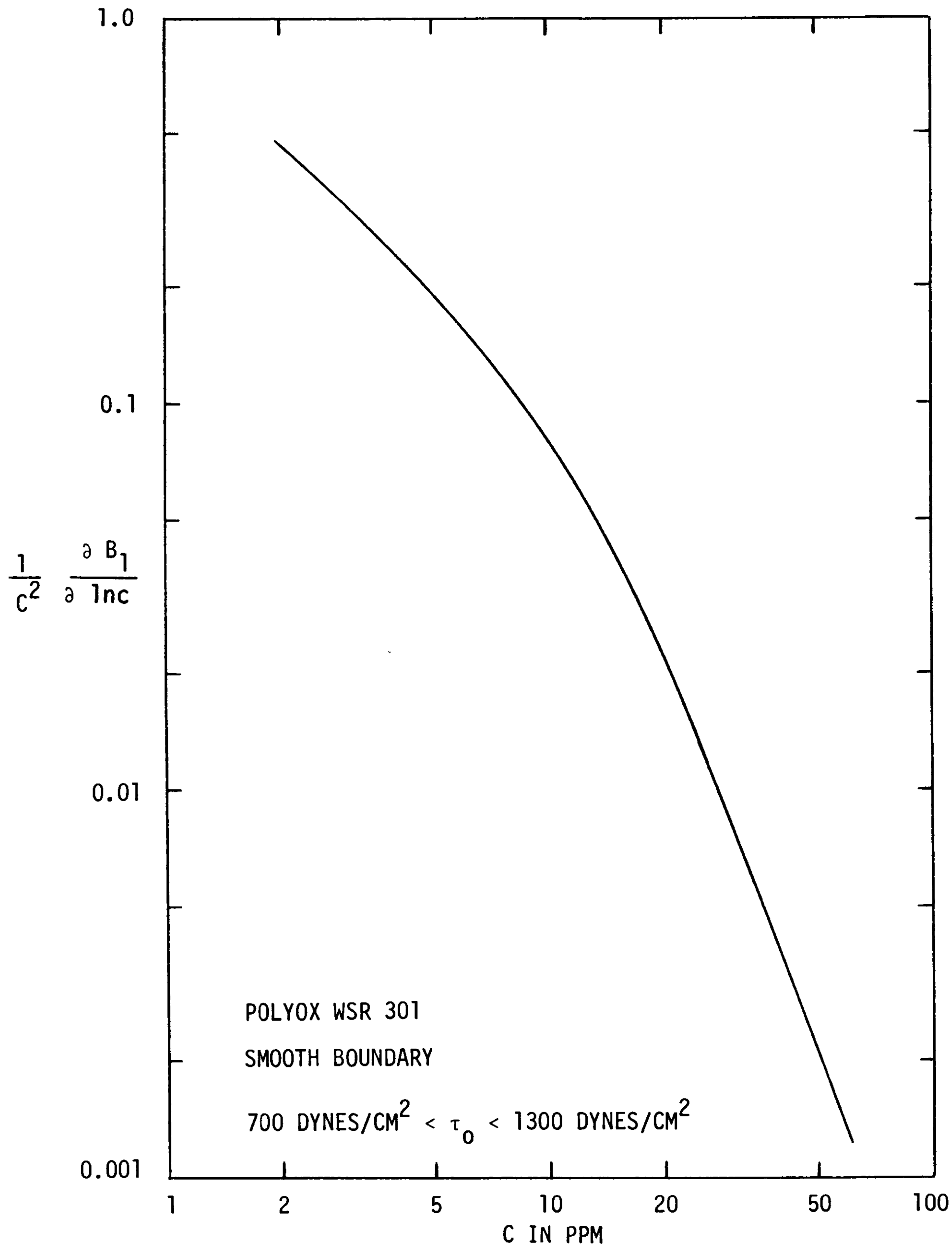

Figure 5 - Calculated Values of $1/c^2 \, \partial B_1/\partial \ln c$ Derived from Figure 2

To determine c_{x_i}, it is first noted that when Equation (34) is evaluated at $x = x_i$, one obtains the following relation between c_{x_i} and σ_{x_i}

$$M_i \cong \frac{\left(C_{F_{x_i}} R_{x_i}\right)_s}{2\,\alpha_o} \sigma_{x_i} c_{x_i} \tag{35}$$

where $(C_{F_{x_i}} R_{x_i})$ is given the subscript s since the frictional drag for $x \leq x_i$ is due to flow of pure solvent. A second relation between c_{x_i} and σ_{x_i}, namely

$$\exp\left\{\frac{1}{A}\left[\sigma_{x_i} - B_1\left(\ell^*_{x_i}, c_{x_i}\right) - B_2\right]\right\} = \frac{\left(C_{F_{x_i}} R_{x_i}\right)_s}{2\,\alpha_o}\left(1 - \frac{\beta_o}{\sigma_{x_i}}\right)^{-1}$$

follows from Equations (5) and (9). Since this expression also holds for pure solvent (subscript s), division by the corresponding solvent equation gives

$$\exp\left\{\frac{1}{A}\left[\sigma_{x_i} - \left(\sigma_{x_i}\right)_s - \Delta B\left(\ell^*_{x_i}, c_{x_i}\right)\right]\right\} = \frac{1 - \dfrac{\beta_o}{\left(\sigma_{x_i}\right)_s}}{1 - \dfrac{\beta_o}{\sigma_{x_i}}}$$

from which one obtains the high order approximation

$$\sigma_{x_i} - \left(\sigma_{x_i}\right)_s \cong \Delta B\left(\ell^*_{x_i}, c_{x_i}\right) \tag{36}$$

Equations (35) and (36) may be used to solve for c_{x_i} and σ_{x_i}, noting that $\ell^*_{x_i} = R_\ell/\sigma_{x_i}$ where $R_\ell = \ell U/\nu o$.

The above completes development of the determination of flat plate frictional drag with polymer injection, subject to the requirement of a vanishingly small intermediate mixing region (i.e., $\mathcal{R}$ = o). For specified ν_o, x, x_i, M_i, B_1 (ℓ*, c) and a number of constants, Equations (31) through (36) may in principle be solved for c_x, σ_x, c_{x_i}, , and C_{F_x}. In practice, it is more convenient to take x and M_i as unknowns and to preassign σ_x and c_x, making use of uniform concentration results. Such a computational scheme will now be outlined.

Consider a given type of polymer solution with ν_o and B_1 (ℓ^*,c) specified. For flat plate flow of the polymer solution at uniform concentration (subscript u), σ_{x_u} and $C_{F_{x_u}}$ may be calculated for given U_u, x_u, and c_u using the method already outlined. In the case of polymer injection (no subscript) at specified x_i, we wish to find the plate length x and polymer supply rate M_i such that $U = U_u$, $\sigma_x = \sigma_{x_u}$, and $c_x = c_u$. (In general $x \neq x_u$.) Now since $\sigma_x = \sigma_{x_u}$ and $c_x = c_u$, it follows from Equation (10), which holds for both uniform and nonuniform concentrations, that $C_{F_x} R_x = C_{F_{x_u}} R_{x_u}$. M_i may then be calculated from Equation (34), and σ_{x_i} and c_{x_i} from Equations (35) and (36). With c_{x_i} determined, the $\mathcal{P}$ integral from Equation (32) may be evaluated, and C_{F_x} follows from Equation (30). The plate length x for polymer injection then follows from the known value of $C_{F_x} R_x$. Repetition of the calculations for various x_u and trailing edge concentrations c_x readily yields curves of C_{F_x} and M_i as functions of U, x, x_i, and c_x.

To illustrate the method outlined above, calculations have been performed for injection of Polyox WSR 301 into salt water at 59 F flowing past a flat plate. The particular case considered was x = 200 ft, x_i = 10 ft, U = 30 knots, and an injected concentration c_i = 2000 ppm. Values used for the constants appearing in the various equations have been taken from References 1 and 4: $A = 2.39$, $\beta_o = 6.64$, $\beta_1 = 5.17$, $\alpha_1/\alpha_o = 0.1603$. In the calculations, ΔB information was obtained from Figures 1, 2, and 5. The required uniform concentration input was taken from Figure 4, and zero concentration input from Reference 14. The final results for polymer injection are plotted in Figures 6 and 7 as a function of trailing edge polymer concentration c_x at the plate surface. Percentage frictional drag reductions (compared to water) are shown in Figure 6 along with the

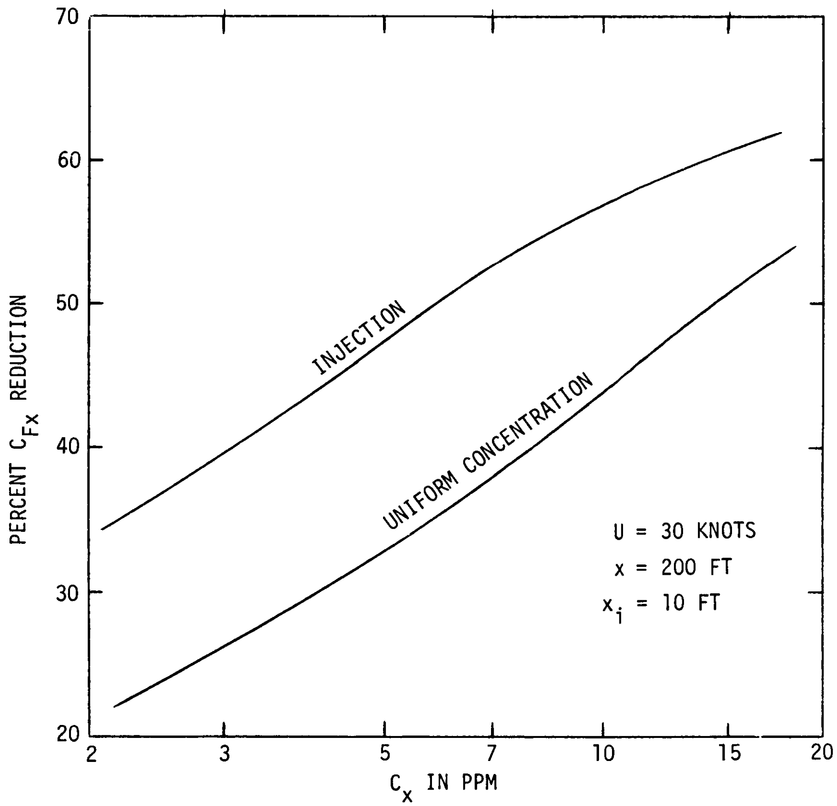

Figure 6 - Example of Predicted Percentage Frictional Drag Reductions for Flat Plate in the Cases of Uniform Concentration and Injection

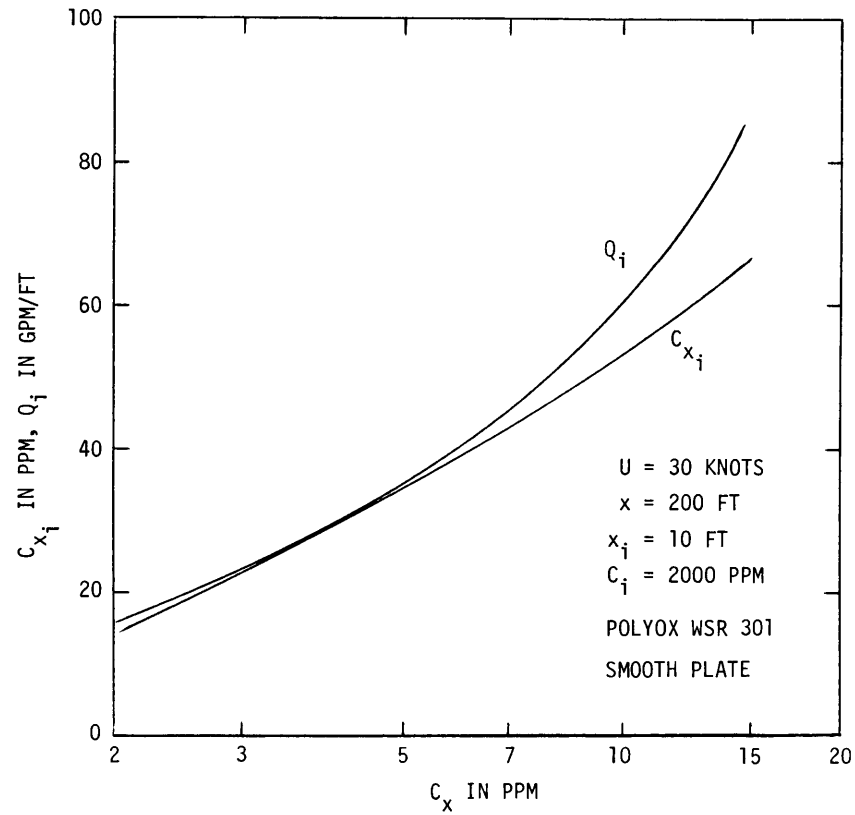

Figure 7 - Predicted Polymer Supply Rates Q_i and Self-Preserving Wall Concentrations c_{x_i} Corresponding to the Injection Case Shown in Figure 6

comparable results from Figure 4 for uniform concentration. Figure 7 gives the corresponding polymer supply rates Q_i and self-preserving wall concentrations c_{x_i} at the injector location x_i.

ACKNOWLEDGMENT

The author is indebted to his friend Paul S. Granville for many valuable discussions on flat plates and polymers.

REFERENCES

1. Granville, P.S., "Frictional Resistance and Velocity Similarity Laws of Drag - Reducing Dilute Polymer Solutions," J. Ship Res., Vol. 12, p. 201 (1968).

2. Fabula, A.G., "Attainable Friction Reduction on Large Fast Vessels," NUWC Tech. Paper 123 (Feb 1969).

3. Wells, C.S. and Spangler, J.G., "Injection of a Drag-Reducing Fluid into Turbulent Pipe Flow of a Newtonian Fluid," The Physics of Fluids, Vol. 10, p. 1890 (1967).

4. Fabula, A.G. and Burns, T.J., "Dilution in a Turbulent Boundary Layer with Polymeric Friction Reduction," AIAA Meeting, Seattle (1969).

5. Granville, P.S., "Drag Reduction of Flat Plates with Slot Ejection of Polymer Solutions," NSRDC Report 3158 (Nov 1969).

6. Ernst, W.D., "Investigation of the Turbulent Shear Flow of Dilute Aqueous CMC Solutions," J. Am. Inst. Chem. Eng., Vol. 12 (1966).

7. Elata, C. et al., "Turbulent Shear Flow of Polymer Solutions," Israel J. Technol., Vol. 4, p. 87 (1966).

8. Virk, P.S. et al., "The Toms Phenomenon; Turbulent Pipe Flow of Dilute Polymer Solutions," J. Fluid Mech., Vol. 30, p. 305 (1967).

9. Meyer, W.A., "A Correlation of the Frictional Characteristics for Turbulent Flow of Dilute Viscoelastic Non-Newtonian Fluids in Pipes," J. Am. Inst. Chem. Eng., Vol. 12 p. 522 (1966).

10. Whitsett, N.F. et al., "Effect of Wall Shear Stress on Drag Reduction of Viscoelastic Fluids," The Western Company, Report DTMB-3, ONR Contract Nonr 4306(00), GHR Program SR 009 01 01 (1968).

11. Wells, C.S., "The Use of Pipe Flow Correlations to Predict Turbulent Skin Friction for Drag-Reducing Fluids," AIAA Meeting, Seattle (1969).

12. Fabula, A.G., "The Toms Phenomenon in the Turbulent Flow of Very Dilute Polymer Solutions," Proc. 4th Intl. Cong. Rheology, Part 3, p. 455 (1965).

13. Goren, Y. and Norbury, J.F., "Turbulent Flow of Dilute Aqueous Polymer Solutions," J. Basic Eng., Series D, Vol. 89, p. 814 (1967).

14. Todd, F.H., "Tables of Coefficients for ATTC Model-Ship Correlation and Kinematic Viscosity and Density of Fresh and Salt Water," SNAME T&R Bulletin 1-25 (1964).

15. Poreh, M. and Cermak, J.E., "Study of Diffusion from a Line Source in a Turbulent Boundary Layer," Intl. J. Heat Mass Transfer, Vol. 7, p. 1083 (1964).

16. Wetzel, J.M. and Ripken, J.F., "Shear and Diffusion in a Large Boundary Layer Injected with Polymer Concentrate," University of Minnesota, St. Anthony Falls Hydraulic Laboratory, Project Report 114, ONR Contract Nonr 710(71) GHR Program SR 009 01 01 (Feb 1970).

INITIAL DISTRIBUTION

Copies

12 NAVSHIPSYSCOM
- 2 SHIPS 2052
- 1 SHIPS 031
- 1 SHIPS 034
- 1 SHIPS 0341
- 1 SHIPS 03412
- 1 SHIPS 0342
- 1 SHIPS 037
- 1 SHIPS 037C
- 1 SHIPS 0372
- 1 SHIPS PMS381
- 1 SHIPS PMS393

2 DSSPO
- 1 Ch Sci (PM 11-001)
- 1 Vehicles (PM 11-22)

3 NAVSEC
- 1 SEC 6110-01
- 1 SEC 6136
- 1 SEC 6114D

3 CHONR
- 2 Fl Dyn Br (ONR 438)
- 1 Chem Br (ONR 472)

3 NAVORDSYSCOM
- 1 Weap Dyn Div (NORD 035)
- 1 Hydro Pro Eng (NORD 05431)

2 NAVAIRSYSCOM
- 1 Aero & Hydro Br (NAIR 5301)

1 CO & DIR, USNUSL (New London)

1 CO & DIR, USNELC (San Diego)

6 CO & DIR, USNOL (White Oak)
- 1 Dr. R.E. Wilson
- 1 Dr. A.E. Seigel
- 1 Dr. A. May
- 1 N. Tetervin
- 1 Dr. V.C. Dawson

7 CDR, USNUWC (Pasadena)
- 1 Dr. J.W. Hoyt
- 1 Dr. A.G. Fabula
- 1 Dr. T. Lang
- 1 Dr. J.G. Waugh
- 1 Dr. W.D. White

1 CDR, NWC (China Lake)

Copies

2 Dir, USNRL (Wash D.C.)
- 1 Dr. R.C. Little (Surf Chem Br)

5 Co, USNAVUWRES (Newport)
- 1 R.J. Grady
- 1 P.E. Gibson
- 1 J.F. Brady
- 1 R.H. Nadolink

1 BUSTDS
Attn: Hydraulic Lab

20 CDR, DDC

1 Lib of Congress (Scl & Tech Div)

1 MARAD

1 CO, U.S. Army Transp R&D Com Fort Eustis, Va. (Mar Transp Div)

1 SNAME
74 Trinity Pl., N.Y. 10006

1 Webb Inst of Nav Arch
Crescent Beach Rd, Glen Cove, L.I., N.Y. 11542

5 ORL, Penn State Univ 16802
- 1 Dr. J.L. Lumley
- 1 Dr. M. Sevik
- 1 R.E. Henderson
- 1 Dr. F.W. Boggs

2 Davidson Lab, Stevens Inst, Hoboken, N.J. 67030
- 1 J. Breslin

2 Alden Res Lab, Worchester, Mass.
- 1 L.C. Neale

2 Univ of Mich, Ann Arbor 48104
- 1 Dept Naval Arch
- 1 W.P. Graebel (Dept Eng Mech)

2 Iowa Inst Hydraulic Res
State Univ of Iowa, Iowa City 62240
- 1 Prof L. Landweber
- 1 Dr. M. Poreh

Copies	
2	Stanford Univ, Stanford, Calif 1 Prof E.Y. Hsu, Dept Civil Eng 1 Prof S.J. Kline, Dept Mech Eng
4	MIT, Cambridge, Mass 02139 2 Dept Nav Arch 2 Dept Chem Eng
1	Prof A.J. Acosta, Hydrodyn Lab Cal Tech, Pasadena, Calif 91109
1	Prof. N.S. Berman, Dept Chem Eng Arizona St Univ, Tempe, Ariz 85281
1	Prof E.F. Blick, Univ of Oklahoma Res Inst Norman, Okla 73069
1	Prof C.E. Carver Jr. Dept of Civil Eng Univ of Mass, Amherst, Mass 01002
1	W.B. Giles, R&D Center Gen Electric Co, Schenectady, N.Y. 12301
1	Prof. H.C. Hershey, Dept of Chem Eng Ohio State Univ, Columbus, Ohio 43210
1	Prof. Bruce Johnson, Eng Dept U.S. Naval Acad, Annapolis, Md. 21402
1	Prof. A.B. Metzner, Dept of Chem Eng Univ of Delaware, Newark, Del 19711
2	Dept of Chem Eng, Univ of Missouri-Rolla Rolla, Mo 65401
3	St. Anthony Falls Hydraulic Lab Univ of Minnesota, Minneapolis, Minn 55414
1	Prof. T. Sarpkaya, Dept of Mech Eng Naval Postgraduate School, Monterey, Calif 93940
2	Univ of Rhode Island, Kingston, R.I. 02881 1 Prof F.M. White, Dept of Mech Eng 1 Prof T. Kowalski, Dept of Ocean Eng
1	Prof E.R. Lindgren, Sch of Eng Univ of Florida, Gainesville, Fla 32601
1	Prof. A.T. McDonald, Sch of Eng Purdue Univ, W. Lafayette, Ind 47907
1	J.G. Savins, Mobil Field Res Lab P.O. Box 900, Dallas, Tex 75221
4	Hydronautics Inc. Pindell School Rd Laurel, Md. 20810 1 V. Johnson 1 Dr. Jin Wu 1 M.P. Tulin

Copies	
1	Dr. E.R. van Driest, Ocean Sys North Av Rockwell Corp 3370 Miraloma Ave, Anaheim, Calif 92803
2	Dr. C.S. Wells, LTV Res Center P.O. Box 6144, Dallas, Tex 75222
1	J. Levy, Hydrodyn Dept Aerojet-Gen, Azusa, Calif
1	A. Lehman, Oceanics, Inc Plainview, L.I., N.Y. 11803
1	Prof. E.M. Uram, Dept Mech Eng Univ of Bridgeport, Bridgeport, Conn 06602
1	Ira R. Schwartz, Fluid Phys Rv (RRF) NASA Hdqtrs, Wash D.C. 20546
1	Prof W. Squire Univ of West Virginia, Morgantown, W. Va.
1	Prof. R.I. Tanner, Dept of Mech Brown Univ, Providence, R.I.
1	Dr. Richard Bernicker Esso Math & Sys Inc Florham Park, N.J.
1	Prof A. Ellis Univ of Calif at San Diego, Lajolla, Calif 92106
1	Prof J.P. Tullis, Dept Civil Eng Colorado State Univ, Fort Collins, Colo 80521
1	Dr. F.W. Stone Union Carbide Corp P.O. Box 65 Tarrytown, N.Y. 10591

☆ U.S. GOVERNMENT PRINTING OFFICE: 1970-397-175/80

UNCLASSIFIED

Security Classification

DOCUMENT CONTROL DATA - R & D

(Security classification of title, body of abstract and indexing annotation must be entered when the overall report is classified)

1 ORIGINATING ACTIVITY (Corporate author) Naval Ship Research and Development Center Washington, D.C. 20007	2a. REPORT SECURITY CLASSIFICATION UNCLASSIFIED 2b. GROUP

3 REPORT TITLE

FLAT PLATE FRICTIONAL DRAG REDUCTION WITH POLYMER INJECTION

4 DESCRIPTIVE NOTES *(Type of report and inclusive dates)*

Final Report

5 AUTHOR(S) *(First name, middle initial, last name)*

Justin H. McCarthy

6 REPORT DATE	7a. TOTAL NO. OF PAGES	7b. NO. OF REFS
April 1970	31	16

8a. CONTRACT OR GRANT NO b. PROJECT NO SF 35421003 Task 01710 c. d.	9a. ORIGINATOR'S REPORT NUMBER(S) 3290 9b. OTHER REPORT NO(S) (Any other numbers that may be assigned this report) AD 706 321

10 DISTRIBUTION STATEMENT

This document has been approved for public release and sale; its distribution is unlimited.

11 SUPPLEMENTARY NOTES	12 SPONSORING MILITARY ACTIVITY
	NAVSHIPS

13 ABSTRACT

A method is developed for prediction of frictional drag reduction in high Reynolds number flows past smooth flat plates with polymer injection near the leading edge. Numerical results are given for water-Polyox WSR 301 solutions with either uniform concentration or injection.

DD FORM 1 NOV 65 1473 (PAGE 1)

S/N 0101-807-6801

UNCLASSIFIED

Security Classification

14 KEY WORDS	LINK A		LINK B		LINK C	
	ROLE	WT	ROLE	WT	ROLE	WT
Drag Reduction						
Polymer Injection						
Flat Plate Frictional Drag						
Smooth Plates						
Boundary Layers (Turbulent)						
Prediction of Frictional Drag						